Balanced Magnetic Antenna for Partial Discharge Measurements in Gas-Insulated Substations

Mier Escurra, Christian; Mor, Armando Rodrigo

DOI
10.23919/CMD54214.2022.9991698

Publication date
2022

Document Version
Final published version

Published in
Proceedings of the 2022 9th International Conference on Condition Monitoring and Diagnosis (CMD)

Balanced Magnetic Antenna for Partial Discharge Measurements in Gas-Insulated Substations

Christian Mier Escurra [1*], Armando Rodrigo Mor [2]

[1] Delft University of Technology

[2] Universitat Politècnica de València

* C.MierEscurra@tudelft.nl

Abstract – **Recent research has found that Magnetic loop antennas can detect partial discharges (PD) in gas-insulated substations (GIS); however, unbalanced shielded loop (UBSL) antennas are affected by electric field coupling. This research proposes a balanced shielded loop (BSL) adapted for GIS PD sensing with different designs. The frequency response and PD charge estimation for BSL and UBSL antennas are analyzed and compared in a matched test bench using a very-fast pulse calibrator. The results confirmed a better common-mode noise rejection and thus a better charge estimation by using the balanced magnetic antenna. An alternative BSL design improved the antenna's gain by a factor of two, and by using a balun transformer, the gain was increased by a factor of 4. The results showed the criticality in the shielded gap placement and the influence of the antenna's parasitic elements on the balun's frequency response. This paper shows an improvement in the noise rejection using magnetic antennas, which leads to the possibility of better PD sensing in GIS.**

Keywords: Partial discharge, gas-insulated substation, GIS, magnetic antenna, common-mode noise, balanced shielded loop.

I. INTRODUCTION

Gas-insulated substations (GIS) exhibit advantages over traditional air-insulated substations: long life span, high reliability, and reduced space, making them worthwhile in remote areas. An electric failure in such outlying sites could compromise the entire substation; therefore, reliable remote monitoring of the GIS's insulation condition is needed. An accepted method for insulation diagnosis is partial discharges (PD) measurements, and in many cases, it is a requirement in the acceptance protocol [1].

Reference [2] shows a novel PD measuring system for GIS, consisting of a magnetic loop antenna (MLA). By measuring with the MLA in the very-high frequency (VHF), it is possible to estimate the PD charge, which indicates the severity of the insulation degradation, and harmonizes readings from different sensors [3]. Further research [4] discusses the interaction of common-mode (CM) currents in MLA and a method to reduce it without eliminating it. The CM current modifies the antenna's transfer function (TF), altering the charge estimation methods dependent on the TF [5].

Balanced shielded loops (BSL) are well known in radio transmission applications and are characterized for having good common-mode rejection [6]; they sense magnetic fields while rejecting electric fields. It is believed that MLAs are affected by CM currents in the same way as in [7], although MLAs for PD measurements in GIS have a different configuration. The MLA presented in previous research [4], [8], [9] consisted of a "lateral-gap" structure, which is a type of unbalanced shielded loop (UBSL).

This paper presents the BSL as a PD sensor in GIS. The CM sensitivity and charge estimation are compared between the BSL and the UBSL, and an alternative BSL antenna, which achieves higher coupling, is presented. Additionally, a balanced to unbalanced transformer (balun) is proposed, increasing the sensor's gain.

II. BALANCED AND UNBALANCED SHIELDED LOOP ANTENNAS

A. Mathematical Model

Previous research showed a magnetic loop antenna for PD measurements in GIS, using a UBSL antenna due to its construction simplicity. Fig.1 (a) shows the UBSL electric diagram [4] and picture, including the transfer function (1) that correctly represents the antenna in a frequency range below 300 MHz, where V_{pd} is the induced PD voltage to the loop, L_s is the loop's self-inductance, R_l is the antenna's load, and l is the length of the transmission line (TL) loop. The model of the BSL antenna is shown in other investigations, resulting in the electric diagram and picture in Fig. 2 b) and the model in (2). The BSL divides the loop into two equal arms, resulting in two outputs with the same equation as the UBSL but with half coupling inductance, half self-inductance, and half TL length.

$$H(\omega) = \frac{-j\omega M e^{-jBl}}{1 + j\omega L_s / R_l} \tag{1}$$

$$H(\omega) = \frac{-j\omega M e^{-jB\,l/2}}{2 + j\omega L_s / R_l} \tag{2}$$

B. Common-mode currents

The magnetic antennas are intended to measure only the magnetic field; however, the electric field is also induced, producing common-mode currents. In the BSL, the common-mode currents are divided equally (same magnitude and phase) in the loop arms, resulting in a zero magnetic field in the loop Fig. 2 a). In the UBSL, each arm has a different length with a different inductance and capacitance, dividing the CM current unevenly and thus, inducing a magnetic field in the loop. Reference [4] proposes the reduction of the CM currents by placing a shock ferrite, where resonances produced at ≈150 MHz were eliminated; however, the influence of the CM current was still present.

"This project 19ENG02 FutureEnergy has received funding from the EMPIR programme co-financed by the Participating States and from the European Union's Horizon 2020 research and innovation programme")

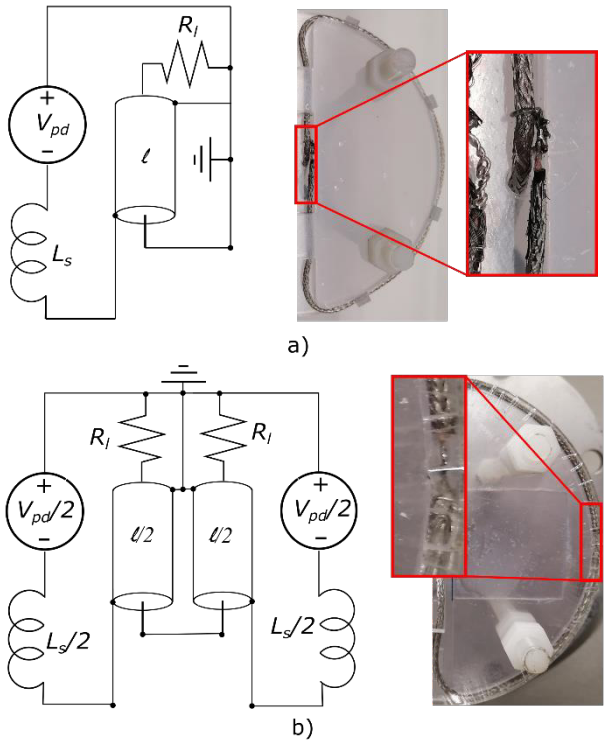

Figure 1. a) UBSL electric diagram and picture with zoomed gap. b) BSL electric diagram and picture with zoomed gap.

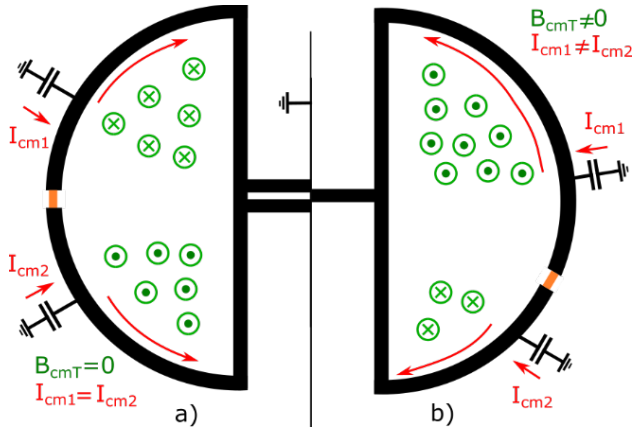

Figure 2. CM-current and induced magnetic field in a) BSL and b) UBSL antennas.

C. Eight-shaped antenna

Equation (2) shows that the BSL's coupling inductance is reduced by half compared to the UBSL. One way to double the BSL's coupling is by increasing the loop area using the complete mounting hole's area; however, this is impossible in a circular loop [2]: the magnetic field has different polarities in each half mounting hole's area. A solution is to build the loop in an "eight" shape; the magnetic field in each half contributes to the total induced electromotive force (EMF). Fig. 3 clarifies the explanation: The PD current (I_{pd}) splits when it encounters the GIS's mounting hole, producing a magnetic field (B_{pd}) with opposite polarity in each half of the mounting hole; the induced EMF results in the same polarity following the eight-shaped path. The noise discrimination method presented in [10] cannot be applied to this solution; it uses two different lobes in the mounting hole.

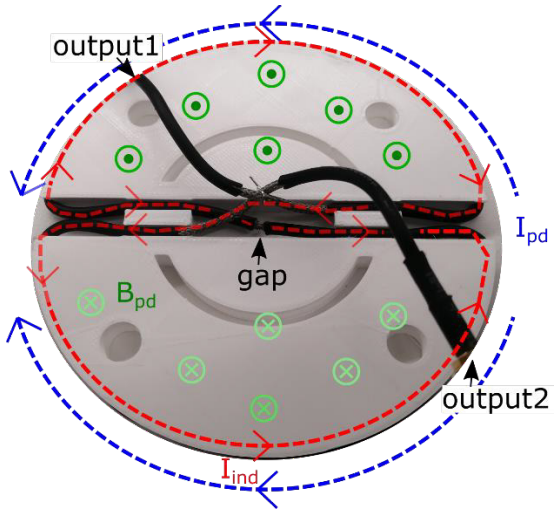

Figure 3. Eight-shaped BSL antenna showing the PD current, the induced magnetic field, the induced current, the outputs and the gap.

D. Balun

The BSL's output voltage (from the inner conductor to ground) is halved with respect to the UBSL's output voltage (unbalanced signal); if the BSL is measured from one output's inner conductor to the other (balanced signal), the magnitude is maintained. Unfortunately, it is impossible to directly measure a balanced signal with a grounded instrument. An alternative is a balun transformer, where special care must be put into the balun's transfer impedance. Fig. 4 shows a balun's diagram, where: Z_0 is the characteristic impedance of the antenna's coaxial cable and is the same for both arms; $V_{1\text{-}2}$ is the balanced voltage, and it is the addition of the arms output voltages V_1 and V_2; V_3 is the unbalanced output of the balun; and Z_3 is the output impedance seen by the balun.

It is crucial to keep the antenna matched; otherwise, unwanted reflections are measured. To match the antennas' outputs, the reflected impedance must be twice the antenna's arm, in this case, 100 Ω, for a 50 Ω coaxial line. The reflected impedance results from the secondary impedance and the number of turns. A 1:1 balun (CoilCraft, WBC1-1TL) was selected for this research since it offers a broader bandwidth, resulting in Z_3=100 Ω. Since Z_3 impedance is different from the 50 Ω of the rest of the measuring system, an amplifier with 100 Ω input and 50 Ω output was designed using an Op-Amp AD8000.

Any transformer is not perfectly coupled, leaving a parasitic inductance in series with the load. The antenna sees this inductance as an unmatched load, resulting in resonances in the frequency domain. The resonance can be shifted to higher frequencies by reducing the antenna's transmission line length before the balun. Equations (1) and (2) are a simplification when the load is matched with the antenna's TL; the model adding the balun inductance can be derived following the procedure in [4].

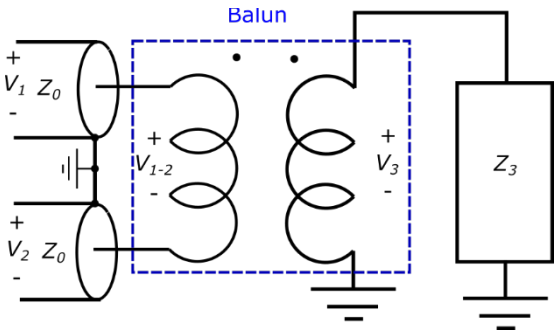

Figure 4. Electric diagram for a balun transformer.

III. Experiments and Results

This research compares the common-mode currents and the charge estimation between the UBSL and BSL. A matched test bench is used to measure the CM currents in the frequency domain and the charge estimation in the time domain. Fig. 5 shows a schematic of the test setup: the frequency domain is measured using a Vector Network Analyzer (VNA) injecting at one cone and terminating the other; for time-domain measurements, a pulse generator is connected to one of the cones and measured with an oscilloscope at the other cone. Reference [11] shows a detailed explanation of the test bench used for GIS antennas.

A. Common-mode currents, eight-shaped BSL and balun

It is hard to measure the CM current in a normal operating condition since the differential signal eclipses it. Reference [2] and [4] demonstrate that if the antenna is rotated 90°, just the CM currents are measured. Fig. 6 shows the frequency response for the UBSL and BSL in normal operation and rotated 90°; the following observations can be extracted from the figure:

- The UBSL shows a higher magnitude in the low-frequency range during normal operation because of the higher couponing inductance.
- When the antennas are rotated 90°, the magnitude of the UBSL is higher than in the BSL. The UBSL CM current is almost 10 % of the differential signal, whereas the signal is about 1 % in the BSL case.
- The BSL measured noise is attributed to the gap not being perfectly centered. Also, even if the antenna is perfectly designed, there are other noise sources unrelated to CM currents [7].

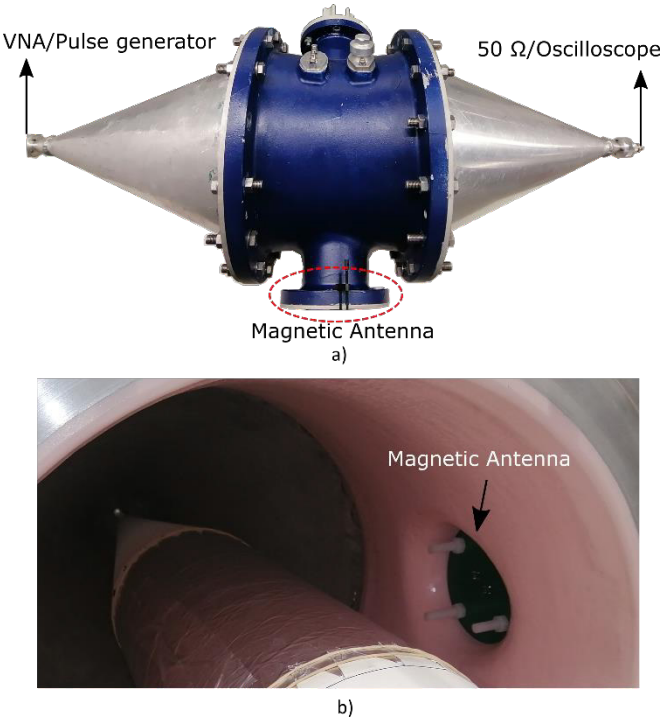

Figure 5. a) Matched test bench for antenna's frequency and time-domain measurements. b) Antenna location seen from inside the test bench.

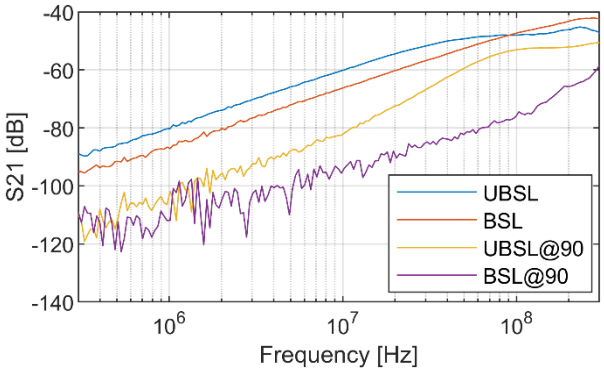

Figure 6. Frequency response for the UBSL and BSL in normal operation and rotated 90°.

Fig. 7 shows the Bode plot of the eight-shaped BSL compared to the single lobe BSL. The eight-shaped antenna has double coupling and double self-inductance than the BSL, giving a frequency response similar to the UBSL antenna, giving the eight-shaped antenna the CM-current characteristic of a BSL with the gain of the UBSL. Higher coupling inductance helps in the calibration constant determination [12].

Fig. 7 also shows the frequency response when using the balun with different transmission line lengths. The BSL with a 24 cm TL length gives a resonance of around 215 MHz; when the distance is decreased to 12 cm, the resonance shifts to 300 MHz. The eight-shaped antenna is twice longer than the BSL giving a TL length of 36 cm; hence, moving the resonance to 150 MHz. For better PD charge estimation, the resonances must be avoided.

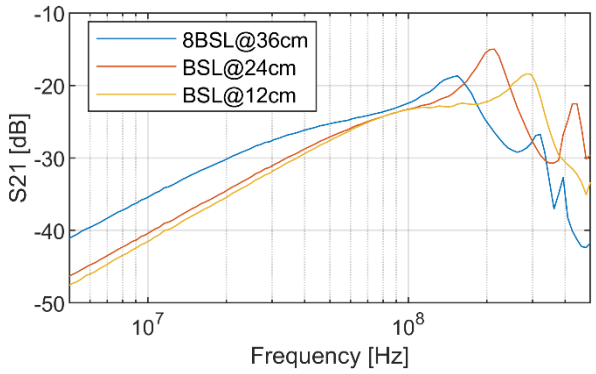

Figure 7. Frequency response for a balun using different TL lengths.

B. PD charge estimation

This section analyzes charge estimation using different antennas and different charge estimation methods. The charge estimation methods are the time-domain (TD), frequency-domain (FD), and voltage double integral (V2I) methods mentioned in [5] and [13]. All antennas were measured with a 190 MHz, 8th order, low-pass filter, and a 25 dB voltage amplifier (when the balun is not used).

Table 1 shows a BSL charge estimation improvement over the UBSL; this is not the case for the "eight-shaped" antenna. The gain is improved when the balun is used; however, the charge estimation error increases, especially with the eight-shaped antenna where the resonance is not filtered.

TABLE I. CHARGE ESTIMATION ERRORS FOR DIFFERENT ANTENNAS AND METHODS.

Antenna	TD error	FD error	V2I error
UBSL	23.0 [%]	13.3 [%]	13.9 [%]
BSL	61.2 [%]	21.6 [%]	1.30 [%]
8BSL	21.3 [%]	11.5 [%]	24.3 [%]
BSL balun	48.7 [%]	26.1 [%]	8.9 [%]
8BSL balun	1.43 [%]	9.03 [%]	30.5 [%]

IV. CONCLUSIONS

The experiments confirmed that the common-mode current is reduced when a BSL is used, resulting in a better charge estimation. The eight-shaped showed a better coupling than the BSL but a higher charge estimation error. Results showed that a balun is a good alternative for increasing the sensor's gain; however, care must be considered for the TL length. This study contributes to the design of VHF magnetic antennas for PD measurements in GIS. The next step is to analyze the BSL antenna using real PD and noisy GIS.

REFERENCES

[1] W. G. D1.25, "UHF partial discharge detection system for GIS: Application guide for sensitivity verification," 2016.

[2] A. Rodrigo-Morz, F. A. Muñoz, and L. C. Castro-Heredia, "A novel antenna for partial discharge measurements in GIS based on magnetic field detection," *Sensors (Switzerland)*, vol. 19, no. 4, 2019, doi: 10.3390/s19040858.

[3] A. Cavallini, G. C. Montanari, and M. Tozzi, "PD apparent charge estimation and calibration: A critical review," *IEEE Trans. Dielectr. Electr. Insul.*, vol. 17, no. 1, pp. 198–205, 2010, doi: 10.1109/TDEI.2010.5412018.

[4] C. Mier, A. R. Mor, and P. Vaessen, "Design and Characterization of a Magnetic Loop Antenna for Partial Discharge Measurements in Gas Insulated Substations," *IEEE Sens. J.*, vol. 21, no. 17, pp. 18618–18625, 2021, doi: 10.1109/JSEN.2021.3089084.

[5] A. R. Mor, P. H. F. Morshuis, and J. J. Smit, "Comparison of charge estimation methods in partial discharge cable measurements," *IEEE Trans. Dielectr. Electr. Insul.*, vol. 22, no. 2, pp. 657–664, 2015, doi: 10.1109/TDEI.2015.7076760.

[6] L. L. Libby, "Special Aspects of Balanced Shielded Loops," *Proc. IEEE*, vol. 34, no. 9, pp. 641–646, 1946.

[7] C. F. M. Carobbi and L. M. Millanta, "Analysis of the Common-Mode Rejection in the Measurement and Generation of Magnetic Fields Using Loop Probes," *IEEE Trans. Instrum. Meas.*, vol. 53, no. 2, pp. 514–523, 2004, doi: 10.1109/TIM.2004.823297.

[8] A. Rodrigo Mor, F. A. Muñoz, J. Wu, and L. C. Castro Heredia, "Automatic partial discharge recognition using the cross wavelet transform in high voltage cable joint measuring systems using two opposite polarity sensors," *Int. J. Electr. Power Energy Syst.*, vol. 117, no. November 2019, 2020, doi: 10.1016/j.ijepes.2019.105695.

[9] C. Mier and A. R. Mor, "Partial Discharge Charge Estimation In Gas Insulated Substations Using Electric and Magnetic Antennas," in *IEEE 2022 International Conference on Dielectrics*, 2022, pp. 1–4.

[10] F. Muñoz-Muñoz and A. Rodrigo-Mor, "Partial discharges and noise discrimination using magnetic antennas, the cross wavelet transform and support vector machines," *Sensors (Switzerland)*, vol. 20, no. 11, pp. 1–14, 2020, doi: 10.3390/s20113180.

[11] C. Mier and A. R. Mor, "Test Bench and Frequency Response of a Magnetic Antenna used in GIS PD Measurements," no. 2, pp. 269–272, 2021, doi: 10.1109/eic49891.2021.9612372.

[12] C. Mier, A. Rodrigo Mor, L. Castro, and P. Vaessen, "Magnetic and electric antennas calibration for partial discharge charge estimation in gas-insulated substations," *Int. J. Electr. Power Energy Syst.*, vol. 141, no. January, p. 108226, 2022, doi: 10.1016/j.ijepes.2022.108226.

[13] A. Rodrigo-Mor, F. A. Muñoz, and L. C. Castro-Heredia, "Principles of charge estimation methods using high-frequency current transformer sensors in partial discharge measurements," *Sensors (Switzerland)*, vol. 20, no. 9, 2020, doi: 10.3390/s20092520.